Eur. Radiol. 7 (Suppl. 2), S51–S55 (1997)

European
Radiology

High resolution magnetic resonance imaging of trabecular structure

S. Majumdar, H. K. Genant

Department of Radiology, University of California, San Francisco, CA 94143, USA

Although bone mineral density is one of the most important contributing factors to bone strength and risk of fracture, studies have shown that changes in bone quality and structure independent of bone mineral density, influence both bone strength and individual risk of fracture. The influence of these other factors is thought to explain at least partially the observed overlap in bone mineral measurements between patients with and without osteoporotic fractures, irrespective of measurement site or technique. Thus, several new emerging techniques have been aimed at quantifying trabecular bone structure in addition to bone density. It is in the context of non-invasive assessment of trabecular bone architecture, that recent efforts have focussed on the development of imaging modalities such as magnetic resonance (MR) imaging. MR is a non-invasive technique, that provides high resolution images in arbitrary planes, as well in three dimensions and may potentially be useful for the quantitative characterization of the trabecular network both in vitro and in vivo at a number of different skeletal sites.

In MR imaging the depiction of trabecular bone is affected by the precise sequence in which the radiofrequency pulses and magnetic field gradients are applied, their specific time intervals, and the details of the imaging sequence used to generate the MR images. Two different classes of imaging sequences, spin-echo based and gradient echo based sequences have been used to obtain images of trabecular bone structure. In spin-echo sequences a 180 degree RF pulse is applied to obtain an echo signal which is then used to generate an image, whereas in a gradient echo sequence a reversal of the magnetic field gradient is used to generate such an echo. Due to the different physical principles that govern image contrast and appearance there are differences between two images obtained with the same resolution, but different imaging sequences. In both spin-echo and gradient echo images the susceptibility (the ability of a material to be magnetized) difference between bone and bone marrow affects the image appearance of trabecular bone. In both spin-echo and gradient echo MR images the apparent size of trabeculae as depicted may show differences compared to their true dimensions [1, 2]. This amplification of trabecular dimensions is more pronounced in gradient echo images, however, it also depends on the echo time, TE, which is used to acquire the image. At short TE times, the effect is not as marked and increases as the echo time increases. With recent advances in the gradient strength available in clinical imaging systems it is possible to obtain high resolution gradient echo images at relatively short TE times (< 10 ms). This considerably reduces the limitations of gradient echo imaging sequences, and also helps increase the achievable signal-to-noise ratio at a given spatial resolution. The advantage of using a gradient echo imaging sequence is that it may be extended to in vivo imaging of the radius, calcaneus, phalanges, as a high resolution three dimensional volume may be acquired in considerably less time than an equivalent volume obtained using spin-echo imaging. Jara et al. [3] have developed a modified spin-echo sequence, which reduces the imaging time, and have used it to obtain images of the phalanges. However, as discussed by these investigators, signal to noise considerations limit the application of this technique to regions of small volumes of interest. The differences in the quantitative estimates of bone structure related parameters measured from spin-echo and gradient echo images have been investigated [4]. It has been shown that although absolute measures of trabecular bone structure differ when measured from spin-echo and gradient echo images, trabecular spacing and number are parameters that are the least affected, and the orientation information obtained from both imaging sequences are identical.

Factors such as the repetition time (TR) selected to obtain an MR image also affect the achievable signal to noise. Increasing TR increases the signal to noise in an image. This however, increases the total scan time. The bandwidth or the total duration during which the MR signal is sampled also affects the signal to noise. The

Correspondence to: H. K. Genant

higher the bandwidth used to sample the MR signal, the shorter the achievable echo time (TE). However, with a higher bandwidth the signal to noise achievable is also lower. Thus, the choice of echo time, bandwidth and scan parameters in MR imaging have to be carefully weighed and adjusted because these factors interact in multiple ways and affect the image appearance, resolution and quality.

In deriving quantitative parameters such as trabecular bone area fraction, trabecular width, etc. one of the primary factors is the accurate segmentation of the bone and bone marrow components. As the image resolution is degraded, the segmentation of the bone and marrow phases becomes complicated due to partial volume averaging effects. The observed density profile at the trabecular bone edge has a transition region between marrow and bone. When the image resolution is comparable to trabecular dimensions the size of this transition zone is not negligible. The trabeculae themselves show variations in density within a slice and thus non-uniformity in signal intensity may be detected within individual trabeculae. In vivo, this is particularly true, since the high resolution MR images have spatial resolutions comparable to trabecular dimensions, and in the slice direction, the resolution is greater than the dimensions of individual trabeculae. As a result of this, the intensity histogram in a region comprising trabecular bone and bone marrow may not be bimodal as one would expect in a two phase model where pixels consist of a single component. In image processing, there is no established technique for measuring the accuracy of any segmentation scheme. Every thresholding scheme has some associated subjectivity which may either be operator dependent or dependent on the automated criteria that are specified in a algorithm. Several techniques may be applied when segmenting high resolution images into bone and bone marrow. An intensity based thresholding scheme based on the histogram of signal intensities [4] and internal calibration techniques [5] have been used but because these schemes are based on a single value it may lead to an apparent thickening of trabeculae or a loss of thinner trabeculae within the same image. An adaptive thresholding or an edge detection scheme in MR images may result in a detection of the heterogeneity of bone marrow in the trabecular spaces, and thus inaccurately classify marrow components as bone. Bayesian estimation techniques, the relative merits and resolution dependence of which remain to be evaluated, have also been proposed recently [6]. After the images have been segmented into two phases, the MR images may be used to calculate standard histomorphometry measures of bone structure such as trabecular bone area fraction, trabecular width, trabecular number, and trabecular spacing using run length analysis methods [7].

Another factor that impacts the absolute quantitation of trabecular bone area fraction, trabecular width and spacing is the image resolution, which if it is comparable to the dimension of the structure to be measured [8], can lead to errors in the estimated dimensions. It is evident that when the image resolution is equivalent to trabecular dimensions, the accuracy of measuring the dimensions of trabecular structure is prone to error, regardless of the segmentation scheme. For example, if the image resolution is 100 μm, and the trabecular dimensions are of the order of 100 μm, an error of 1 pixel may potentially be reflected as a 100 % error in the estimated trabecular width. Similarly a trabeculum that is 50 μm thick will still be detected as a 100 μm structure. Thus since the standard stereology measures derived from such MR images reflect an average over a finite resolution that the measures have been denoted as apparent measures such as the apparent trabecular bone area fraction (app BV/TV), trabecular width (app TbTh), trabecular number (app TbN), and trabecular spacing (app TbSp), etc. In addition to standard two dimensional measures of trabecular bone architecture, the connectivity of the trabecular network, as determined from the Euler number [9] or the complexity of the network as determined from extensions of fractal based box-counting techniques [10] may also be used to characterize trabecular bone structure from MR images.

Hipp et al. have compared the MR derived stereology measures, determined from isotropic image voxels of 50 μm, to those obtained using optical imaging and found good correlations [11], while Chung et al. [12] have compared the apparent BV/TV determined from MR images to those determined using displacement techniques and also found good correlations between the two measures. In a recent study using high resolution MR, Antich et al. have confirmed that MR techniques may be used to monitor changes in trabecular bone structure after fluoride therapy using specimen from iliac crest biopsies [13]. The relationship between the MR derived measures of trabecular structure obtained from images of distal radius cubes at resolutions comparable to those that may be obtained in vivo ($156 \times 156 \times 300$ μm) have been compared to those obtained from higher resolution 3D X-ray tomographic microscopy images (XTM) obtained at an isotropic resolution of 18 μm using cubes from human radii [4]. In the MR images, partial volume effects result in an overestimation of trabecular bone area fraction, trabecular width (~ 3 times), and an under estimation of trabecular spacing (~ 1.6 times) when compared to the 18 μm XTM images. A comparison of the MR derived measures with the bone mineral density (BMD) measured using dual X-ray absorptiometry (DXA) shows that trabecular width, area fraction, number increases, while trabecular spacing decreases, as the bone mineral density increases. The correlation between bone mineral density and the measures of trabecular structure are also good. In the radius cubes, the biomechanical elastic modulus in the three orthogonal directions, corresponding to the anatomical distal-proximal (E_{D-P}), anterior posterior (E_{A-P}), and medial-lateral (E_{M-L}), showed correlated differently with the structural parameters (Table 1). A preliminary bivariate analysis model based on whether the improved coefficient of determination, r^2, being significant ($p < 0.1$), showed that the trabecular number and spacing contributed to an improvement in the pre-

Table 1. Correlation (r) and significance (p) between BMD (gm/cm^2), E_{D-P}, E_{M-L}, E_{A-P} and the mean elastic modulus (E) and some of the measures of trabecular structure derived from MR images

	BMD	E_{D-P}	E_{M-L}	E_{A-P}	E
app BV/TV r, p	0.87	0.84, 0.03	0.93, 0.006	0.71, 0.12	0.96, 0.002
app TbTh r, p	0.83	0.63, 0.18	0.68, 0.13	0.81, 0.05	0.82, 0.05
app TbSp r, p	0.87	0.90, 0.02	0.98, 0.008	0.55, 0.26	0.95, 0.003
app TbN r, p	0.71	0.84, 0.03	0.91, 0.01	0.22, 0.85	0.78, 0.06

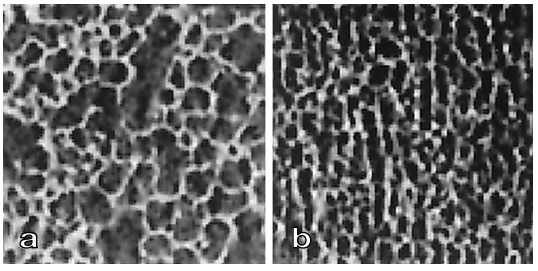

Fig. 1 a, b. High resolution magnetic resonance images clearly depict trabecular bone structure and can be used for quantifying the three dimensional trabecular architecture. **a** Spine; **b** femur

diction of the elastic modulus, compared to bone mineral density alone.

In Fig. 1 reverse gray scale (bone shown in white) MR images at a spatial resolution of $117 \times 117 \times 300$ μm is shown for two specimens, one from the lumbar spine and the other from the proximal femur. The structural features of the trabecular bone at these two sites are quite different as is clearly shown. In all specimens studied the primary orientation of the trabeculae was in the superior-inferior direction. This structural anisotropy was also reflected in the measured elastic modulus which was the highest in the superior-inferior (E_{S-I}) direction. The elastic modulus in the medial-lateral (E_{M-L}) and anterior-posterior (E_{A-P}) showed considerable variations. From such images the three dimensional anisotropy of spine and femur have been determined using software provided by Simmons and Hipp [14]. The binarized images can be used to determine the three dimensional distribution of mean intercept lengths for such cubes. The mean intercept length in 3D generates an ellipsoid, the principal axis of which determines the primary trabecular orientation. The ratio of the principal axes gives the degree of anisotropy in the trabecular bone structure.

With the recent advances in MR imaging hardware and software, it has become possible to obtain high resolution MR images with in-plane resolutions starting at 78 μm and slice thicknesses of 300 μm. Such high resolution images have been obtained in the phalanges by Jara et al. [3], in the distal radius [10], and calcaneus [5, 15]. In a recent in vivo study, high resolution MR images of the distal radius were obtained at 1.5 Tesla in pre-menopausal normal (group I), post-menopausal normal (group II), and post-menopausal osteoporotic group (III) women. The women in groups II and III were also classified as being osteoporotic based on the T-scores [16] of their distal radius BMD determined using peripheral quantitative tomography (pQCT). Representative MR images are shown in Fig. 2.

The MR images were used to derive measures of trabecular bone structure which included apparent measures of trabecular bone area fraction, trabecular thickness, trabecular spacing, trabecular number, etc. Apparent trabecular bone area fraction, app BV/TV, decreased with age, although it showed lower correlations with age, while the app TbN showed moderate correlations and decreased with age. The app TbSp showed the greatest increase and moderate correlation with age. The correlation coefficient and the level of significance for the age app TbTh was low, and the trend of variation of trabecular thickness with age was thus inconclusive (Table 1).

Trabecular bone BMD in the distal radius, app BV/TV, app TbTh, app TbN had the expected trend: i. e. the mean values were the greatest in subjects in group I, decreased progressively in the post-menopausal group (group II), and were the lowest in the post-menopausal osteoporotic group (III). The app TbSp was greatest in group III and lowest in group I. One tailed t-tests were used to assess differences between the density and struc-

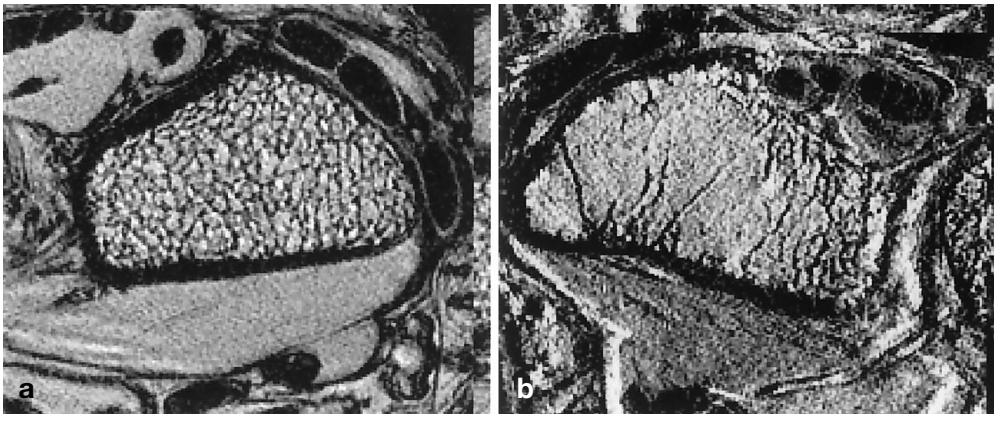

Fig. 2. Representative images from the distal radius of a young normal (**a**) and an elderly osteoporotic subject (**b**) clearly depit the loss of trabecular bone structure in the elderly subject

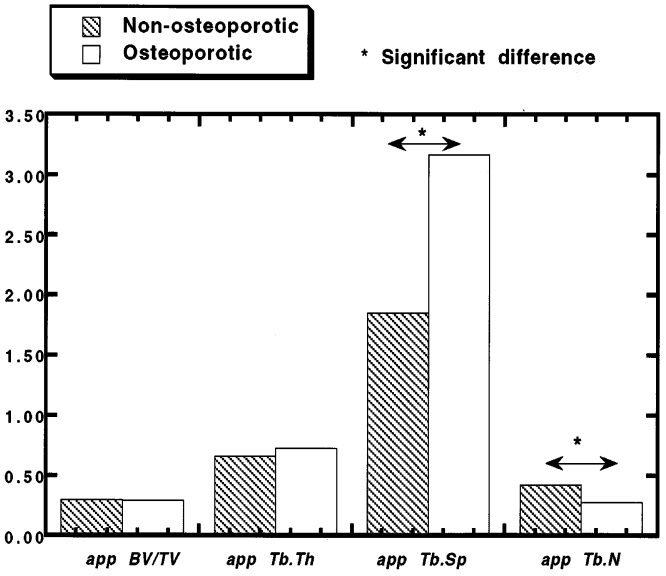

Fig. 3. Differences in the trabecular bone structure parameters between the post-menopausal subjects stratified into two groups based on their osteoporotic status as defined by the World Health Organization [16], i.e. T-Score trabecular BMD < –2.5 was osteoporotic

Table 2. Linear regression was used to determine the change in bone mineral density and the indices of trabecular bone structure as a function of age. The percent change is calculated relative to the 30 year level. The correlation coefficient (r) and the significance level (p) are shown

Parameter	Change (%)	Correlation (r)	Significance (p)
Trabecular BMD pQCT (mg/cm^3)	– 0.61845	0.48	0.007
app BV/TV	– 0.48335	0.33	0.05
app TbTh (mm)	– 0.22780	0.17	0.32
app TbSp (mm)	1.9797	0.50	0.003
app TbN (mm^{-1})	– 0.68146	0.53	0.001

ture parameters in the post-menopausal group (group II and III). Significant differences existed between the fracture and the non-fracture groups in the measured radial trabecular BMD, trabecular bone area fraction, trabecular spacing and trabecular number. The differences in the structural parameters between the subjects classified as osteoporotic based on the WHO [16] definition of osteoporosis and those who were non-osteoporotics is shown in Fig. 3. The app TbN and app TbSp showed significant differences ($p < 0.05$ in a one tailed t-test) between those two groups.

Similarly, magnetic resonance imaging applied to the quantitative measurement of age-related changes in calcaneal trabecular structure from MR images at a spatial resolution of ~ 200 × 200 × 1000 μm, showed that the trabecular structure parameters and age were significantly ($p < 0.05$) correlated: app BV/TV ($r = 0.58$), app TbTh ($r = 0.52$), app TbSp ($r = 0.54$) [5]. The annual rate of change in a normal population was –0.22 %/year, –0.55 %/year, and +1.37 %/year, for app BV/TV, app TbTh and app TbSp respectively. Linear regression analysis also showed significant correlation between the MR-derived trabecular structure parameters and calcaneal BMD values. With improved phased array coils the achievable image resolution in images of the calcaneus now may be as high as 156 μm in plane and 500 μm in slice thickness. Representative axial and sagittal images through the calcaneus are shown in Fig. 4, in reverse gray scale.

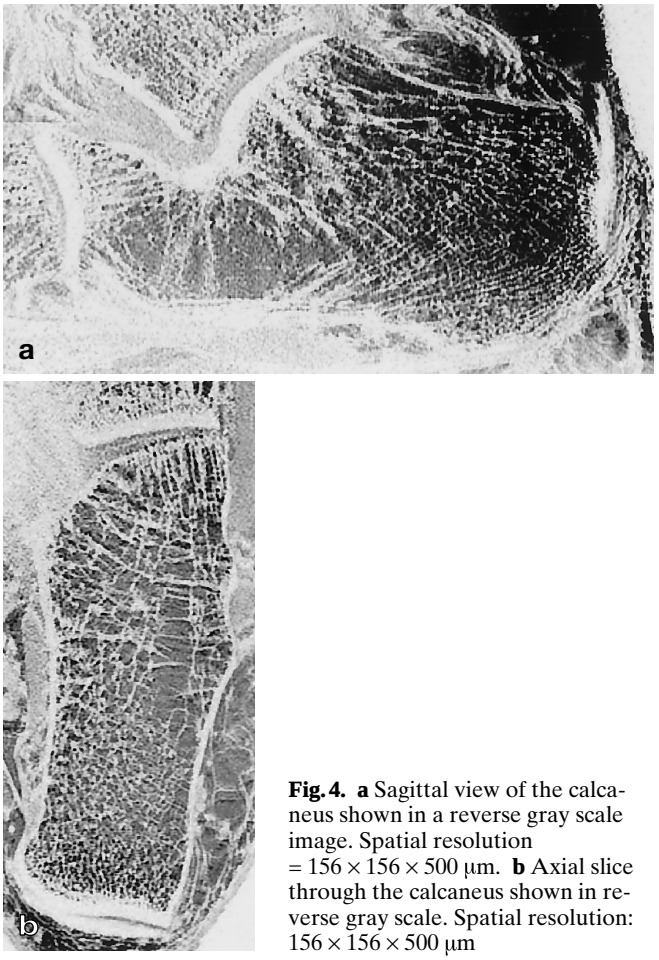

Fig. 4. **a** Sagittal view of the calcaneus shown in a reverse gray scale image. Spatial resolution = 156 × 156 × 500 μm. **b** Axial slice through the calcaneus shown in reverse gray scale. Spatial resolution: 156 × 156 × 500 μm

The heterogeneity of trabecular structure in the calcaneus is evident from the images. In the calcaneus, the highest app BV/TV is seen in the superior region and the lowest in the anterior region. App TbN is highest in the posterior region and lowest in the anterior region. The highest app TbSp is in the anterior region and the lowest in the superior region. Conversely, app TbTh is highest in the superior region and the lowest in the anterior region. For the posterior aspect of the calcaneus, the mean structural parameters as well as BMD within the posterior region, are shown in Table 3. In the posterior part of the calcaneus, in 12 normal subjects, the heterogeneity or percentage variation is 41.7 % for bone fraction while for trabecular number, trabecular spacing, and trabecular thickness it is 21.8 %, 46.0 %, and 42.5 % respectively. The percentage variation for BMD determined in the posterior part

Table 3. Mean ± standard deviation, for the structural parameters, as well as BMD values in the posterior region of the calcaneus for normal subjects (mean age = 38 ± 7 years)

Structure parameter	Mean ± SD
app BV/TV (%)	41 ± 11
app TbN (mm^{-1})	0.82 ± 0.1
app TbSp (mm)	0.81 ± 0.33
app TbTh (mm)	0.50 ± 0.16
BMD (g/cm^2)[a]	0.71 ± 0.09

[a] $n = 10$

(for $n = 8$ subjects) of the calcaneus is considerably lower (~ 11 %).

The advances in magnetic resonance imaging combined with image processing techniques have potential in vitro and in vivo applications in the study of trabecular bone architecture, its' relationship to bone biomechanics and applications to studies of osteoporosis and fracture risk prediction. The non-invasive, three dimensional nature of MR, as well as its ability to predict bone marrow characteristics makes it particularly useful for in vivo studies. It is a new and developing field and further studies are necessary. Hardware and software improvements are needed, particularly in order to extend its application to the spine and proximal femur.

References

1. Bhagwandien R, Moerland MA, Bakker CJ, Beersma R, Lagendijk JJ (1994) Numerical analysis of the magnetic field for arbitrary magnetic susceptibility distribution in 3D. Magn Reson Imag 12: 101
2. Jara H, Wehrli FW (1994) Determination of background gradients with diffusion MR imaging. J Mag Reson Imag 4: 787
3. Jara H, Wehrli FW, Chung H, Ford JC (1993) High-resolution variable flip angle 3D MR imaging of trabecular microstructure in vivo. Magn Reson Med 29: 528
4. Majumdar S, Newitt DC, Mathur A, Osman D, Gies A, Chiu E, Lotz J, Kinney J, Genant HK (1996) Magnetic resonance imaging of trabecular bone structure in the distal radius: relationship with X-ray tomographic microscopy and biomechanics. Osteoporos Int 6: 376
5. Ouyang X, Selby K, Lang P, Engelke K, Klifa C, Zucconi F, Fan B, Hottya G, Majumdar S, Genant HK. High resolution MR imaging of the calcaneus: age-related changes in trabecular structure and comparison with DXA measurements. Calcif Tissue Int (in press)
6. Wu Z, Chung H, Wehrli F (1993) Sub-voxel tissue classification in NMR microscopic images of trabecular bone. Proceedings of the Society of Magnetic Resonance in Medicine: 451
7. Goulet RW, Goldstein SA, Ciarelli MJ, Kuhn JL, Brown MB, Feldkamp LA (1994) The relationship between the structural and orthogonal compressive properties of trabecular bone. J Biomech 27: 375
8. Flynn MJ, Reimann DA (1994) 3D measurement of trabecular architecture with microtomography: dose and resolution. Bone Miner 25: S4
9. Feldkamp LA, Goldstein SA, Parfitt AM, Jesion G, Kleerekoper M (1989) The direct examination of three-dimensional bone architecture in vitro by computed tomography. J Bone Miner Res 4: 3
10. Majumdar S, Genant HK, Grampp S, Jergas MD, Newitt DC, Gies AA (1994) Analysis of trabecular bone structure in the distal radius using high resolution MRI. Eur Radiol 4: 517
11. Hipp JA, Jansujwicz A, Simmons CA, Snyder B (1996) Trabecular bone morphology using micro-magnetic resonance imaging. J Bone Miner Res 11: 286
12. Chung HW, Wehrli FW, Williams JL, Wehrli SL (1995) Three dimensional nuclear magnetic resonance micro-imaging of trabecular bone. J Bone Miner Res 10: 1452
13. Antich PP, Mason RP, McColl R, Zerwech J, Pak CYC (1994) Trabecular architecture studies by 3D MRI microscopy in bone biopsies. J Bone Miner Res 9 [Suppl 1]: 327
14. Simmons C, Hipp JA(1996) Three dimensional mean intercept length ellipsoid software, T3M (personal communications)
15. Majumdar S, Genant HK, Gies AA, Guglielmi G (1993) Regional variations in trabecular structure in the calcaneus assessed using high resolution magnetic resonance images and quantitative image analysis. J Bone Miner Res 8 [Suppl]: 351
16. WHO (1994) Technical report: assessment of fracture risk and its application to screening for postmenopausal osteoporosis: a report of a WHO study group. World Health Organization, Series 843